20th International Conference
ENGINEERING MECHANICS 2014
Svratka, Czech Republic, 12 – 15 May 2014

# INTRA-VOXEL MICRO-ELASTO-PLASTICITY FOR CT-BASED PATIENT-SPECIFIC FRACTURE RISK ASSESSMENT OF VERTEBRAE

**R. Blanchard[*], C. Morin[**], A. Vella[***], Z. Sant[****], Ch. Hellmich[*****]**

**Abstract:** *Following previous studies employing X-ray physics and continuum micromechanics in order to retrieve voxel-specific elastic properties from Computed Tomographs (CT) (Hellmich et al., 2008), we here present an updated and improved approach applied to in-vivo images of vertebrae of a young patient. This approach concerns both elasticity and strength, and therefore promises considerable impact on patient-individual, image-based fracture risk assessment. This is done for the described voxel-specific heterogeneous case, as well as for vascular porosities averaged over the trabecular core. Homogeneous simulations obviously underestimate the fracture risk in the presently studies case.*

**Keywords: Continuum micromechanics, Finite Element model, Spine, Bone strength.**

## 1. Introduction

We here present a novel approach for a patient-specific failure risk assessment from in-vivo CT (Computer Tomography) images. This approach is directly based on the fundamentals of X-ray physics and those of applied micromechanics. Extending the methodology for relating CT data to voxel-specific elasticity in bone (Hellmich et al., 2008; Blanchard et al., 2013) and in biomedical materials for transplants (Scheiner et al., 2009, Dejaco et al., 2012), we here convert information from an in-vivo CT scan of a young patient into voxel-specific bone strength properties by means of a multiscale continuum micromechanics strength model (Fritsch et al., 2009). These properties are then mapped onto a Finite Element mesh, which allows for assessing the effect of material inhomogeneity of bone on the overall structural behavior of the organ. In this context, it is of particular importance to reproduce the morphology of the vertebral body in patient-specific applications, particularly in cases of certain spine pathologies such as scoliosis, where the heterogeneity in bone density within the organ is very important. Therefore, the consideration of patient-specific and spatial heterogeneity within the bone is crucial for medical application.

## 2. Methods

A CT scan of a motion segment of a 15-years-old male patient, consisting of two lumbar vertebral bodies L3 and L4 was obtained from Mater Dei Hospital, Malta. The HiSpeed Dual medical CT scanner from General Electrics in helical mode was employed with the following parameters: source voltage: 140 kV, source current: 110 μA, exposure time: 1000 ms, image pixel size: 0.324 mm, slice spacing: 1.25 mm. The resulting DICOM images were then processed by means of a drawing software in order to capture the geometry of the structure and transported into a Finite Element analysis commercial software. The model has been already utilized in the work published by one of the co-author (Sant et al., 2012). For our purpose, the lumbar vertebral body L3 was isolated from the segment. In these CT images, capturing not

[*] Romane Blanchard: Vienna University of Technology, Institute for Mechanics of Materials and Structures, Karlsplatz 13/202, A-1040, Vienna, Austria, romane.blanchard@tuwien.ac.at
[**] Claire Morin: Ecole Nationale Supérieure des Mines, CIS-EMSE, CNRS:UMR 5307, LGF, F-42023, Saint-Etienne, France, claire.morin@emse.fr
[***] Alain Vella: Mechanical Engineering Department, University of Malta, Tal Qroqq; MSD2080, Msida; Malta, (Imperial College London, Great Britain), carmel.v86@gmail.com
[****] Dr. Ing. Zdenka Sant: Mechanical Engineering Department, University of Malta, Tal Qroqq; MSD2080, Msida; Malta, zdenka.sant@um.edu.mt
[*****] Prof. Christian Hellmich: Vienna University of Technology, Institute for Mechanics of Materials and Structures, Karlsplatz 13/202, A-1040, Vienna, Austria, christian.hellmich@tuwien.ac.at

only the bone structure of a vertebral body, but also the surrounding soft tissue, the X-ray attenuation information is stored in terms of 8-bit grey values, increasing with intensifying attenuation. In order to separate soft and hard tissues, we perform a statistical analysis of the voxel-specific attenuation information leading to the histogram depicted in Fig. 1a.

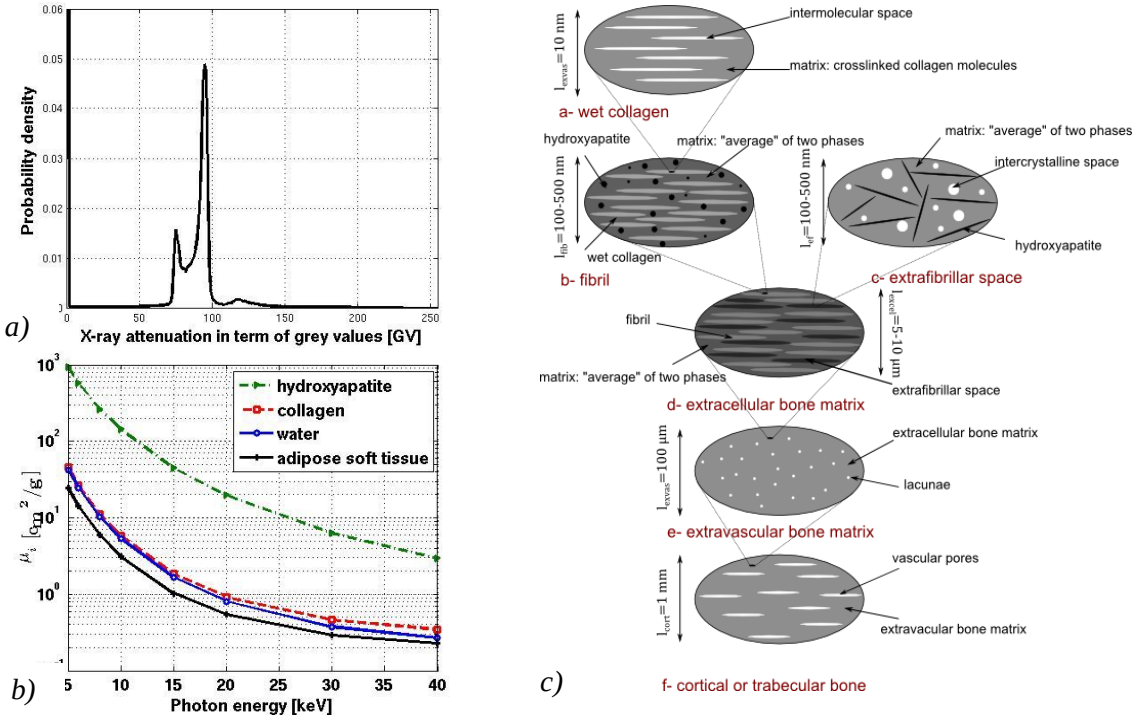


*Fig. 1: a) Frequency distribution plot of the attenuation information in terms of grey values of the vertebral body L3; b) X-ray attenuation coefficients of the elementary constituents of bone tissue, as function of the photon energy; c) Multiscale micromechanical representation of bone material, similar to Fritsch et al. (2009).*

As a first step, we translate the attenuation information in terms of grey values contained in each of the 0.324 mm - sized voxels building up the computed tomograph, into voxel-specific vascular porosity values. Therefore, we consider the linear relation between grey values and X-ray energy-dependent attenuation coefficients, involving three unknowns (two linearity constants and the X-ray energy). The latter are obtained from three known attenuation-energy relationships related to three characteristic points found in the grey value histogram: (i) the left-most peak in this histogram relates to fatty physiological fluid, at $GV_{adipose}$= 70, (ii) the central peak relates to soft tissues as found in the inner organs around the spine, at $GV_{soft}$= 90, and (iii) the densest voxel in the image relates to compact bone with quasi-zero vascular porosity, at GV = 255. The energy-dependent attenuation coefficient of fat is documented in the NIST-database (NIST, n.d.). The latter also gives access to the energy-dependent attenuation coefficients of collagen and water, and their volume ratio in soft tissue [which can be gained from their mass densities and that of soft tissue (Mast, 2000)]. The volume ratio, in turn, in conjunction with the average rule for attenuation coefficients, gives access to the attenuation coefficient of soft tissue.

Also the attenuation coefficient of compact bone is retrieved from averaging the attenuation coefficients of collagen, water, and hydroxyapatite, according to their volume fractions in vertebral extracellular bone matrix. The latter follows from the mass density of extracellular bone matrix in vertebrae (Malandrino et al., 2012), and the averaging of collagen, water, and hydroxyapatite mass densities according to the composition rules evidenced in Vuong and Hellmich (2011).

At the extravascular level, the average rule is written for an RVE of extravascular bone tissue composed of extracellular bone matrix and water-filled lacunar porosity, see Fig. 1c. The attenuation coefficient for extravascular bone matrix enters the average rule for an RVE of macroscopic bone made of extravascular bone matrix and the water-filled vascular porosity; see Fig. 1c. Knowing the attenuation coefficient at each and every grey value, we compute the grey-value-specific porosity.

The vascular porosity values, obtained in this way, enter a continuum micromechanics model for bone (Morin and Hellmich, 2013), which thereupon delivers voxel-specific elastic properties. The tissue mass densities can then be related to the Young's modulus, to the Poisson's ratio, and to the transverse shear modulus.

The latter are mapped onto a 3D Finite Element mesh developed from the same patient data (Sant et al., 2012), consisting of solid elements representing the trabecular bone material, and of shell elements representing cortical bone material. In order to investigate the effect of introducing material heterogeneity into the Finite Element simulation, we build two models: one so-called homogeneous model, with trabecular tissue having homogeneous material properties, namely the elastic properties of the average grey value present in the organ, and one model, so-called heterogeneous model, with element-specific elastic properties. In the latter case, the voxel-specific density is associated to the finite elements by a barycentric-based in-house algorithm. A distributed unit load of 1 MPa is applied onto the upper surface of the third lumbar vertebral body, corresponding anatomically to the upper endplate. The corresponding stress and strain distributions are computed throughout the organ.

These stress states are fed into a six-scale strength up-scaling model for bone, namely an algorithmically stabilized and physically improved version of (Fritsch et al., 2009), as to compute the element-specific proportionality factors by which the actual stresses are multiplied to reach the material yield or failure.

## 3. Results

The voxel-specific intertrabecular porosity and the elasticity reflect the very inhomogeneous nature of the investigated vertebra, see Fig. 2: The left side of the organ is less porous, and hence, denser and stiffer than the right side of the organ.

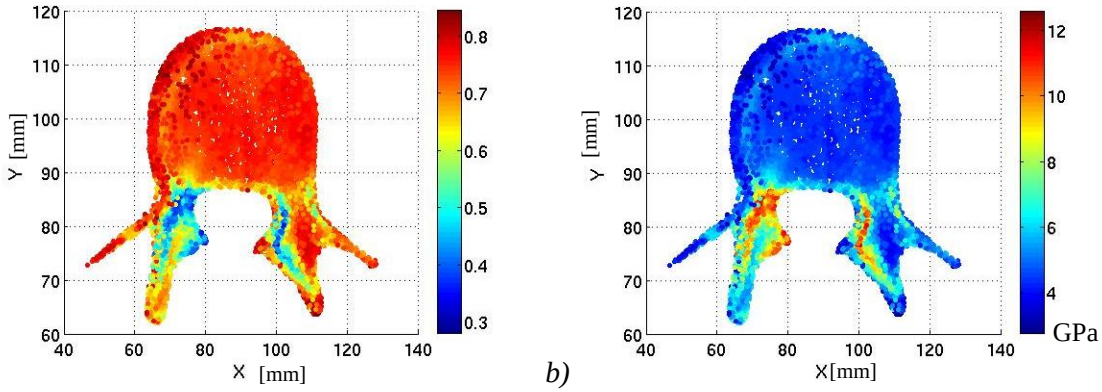


*Fig. 2: Porosity and stiffness maps in a cross section of the Finite Element model, oriented orthogonal to the superior-inferior direction: a) Vascular porosity and b) Axial Young's modulus.*

The factors by which the element-specific stresses, resulting from the 1 MPa pressure loading on the organ, needed to be proportionally magnified to reach the yield point of this element are shown in Fig. 3; which also allows for the comparison of the homogeneous and heterogeneous cases. These factors are directly quantifying fracture risk, on the rigorous basis of engineering mechanics; even for load cases of different magnitude, such e.g. 2 MPa pressure. For the latter case, the yield factors of Fig. 3 needed to be multiplied by ½.

The analysis of the results shows that the first plastification (related to the minimum yield factor) occurs inside the cortical shell in both models, in only two finite elements located near the cranial endplate; this is consistent with the location of high risk of initial failure observed by Eswaran (2007). The second observation is that most of the plastification occurs inside the trabecular core, which is consistent with the observation of microcracks in the trabecular core (Fyrhie and Schaffler, 1994).

As regards the difference between homogeneous and heterogeneous models, the use of a homogeneous model induces an overestimation of the elastic properties and an underestimation of the yield in the organ (see Fig. 3), as well as it neglects the patient-specific heterogeneity of the bony organ created by bone remodelling induced by everyday loads on the spine.

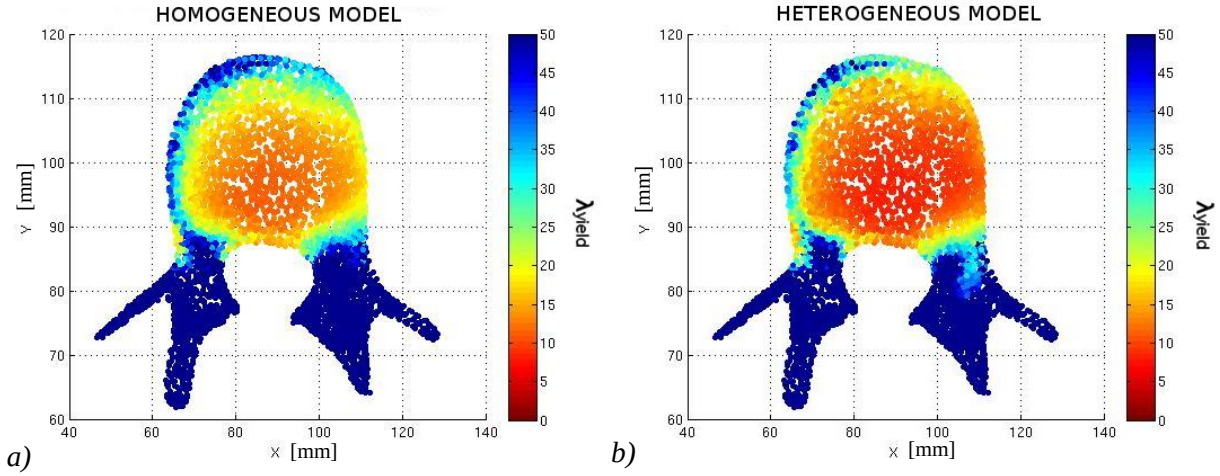


*Fig. 3: Maps of the dimensionless yield factor related to 1 MPa pressure loading, shown across a cross section through the vertebral body, for: a) Homogeneous; b) Heterogeneous Finite Element model, undergoing a unit pressure loading.*


## Acknowledgement

Vertebra modelling was supported by the European Union Seventh Programme (FP7-ICT-2009-6) under the grant agreement number 269909, MySPINE; multiscale strength predictions became possible through the European Research Council (ERC), through the Project MICROBONE, grant number 257023, and the cooperation between Malta and Vienna is an outgrowth of COST Action MP1005, NAMABIO.


## References


Blanchard, R., Dejaco, A., Bongaers, E. & Hellmich C. (2013) Intravoxel bone micromechanocs for microCT-based Finite Element simulations. Journal of Biomechanics, 46(15), pp. 2710-2721.

Crawley, E., Evans, W. & Owen, G.M. (1988) A theoretical analysis of the accuracy of single-energy CT bone measurements, Physics in Medicine and Biology. 33(10), pp. 1113-1127.

Dejaco, A., Komlev, V., Jaroszewicz, J., Swieszkowski, W. & Hellmich C. (2012) MicroCT-based multiscale elasticity of double-porous (pre-cracked) hydroxyapatite granules for regenerative medicine. Journal of Biomechanics, 45(6), pp. 1068-1075.

Eswaran, S.K., Gupta, A., Keaveny, T.M. (2007) Locations of bone tissue at high risk of initial failure during compressive loading of the human vertebral body. Bone, 41(4), pp. 733-739.

Fritsch, A., Hellmich, C., Dormieux, L. (2009) Ductile sliding between mineral crystals followed by rupture of collagen crosslinks: experimentally supported micromechanical explanation of bone strength. Journal of Theoretical Biology, 260, pp. 230–252.

Fyhrie, D.P. and Schaffler M.B. (1994) Failure mechanisms in human vertebral cancellous bone. Bone, 15(1), pp. 105-109.

Hellmich, C., Kober, C. & Erdmann, B. (2008) Micromechanics-based convertion of CT-data into anisotropic elasticity tensors, applied to FE simulations of a mandible. Annals of Biomedical Engineering, 36(1), pp. 108-122.

Malandrino, A. Fritsch, A., Lahayne, O., Kropik, K., Redl, H. Noailly, J., Lacroix, D., & Hellmich, C. (2012) Anisotropic tissue elasticity in human lumbar vertebra, by means of coupled ultrasound-micromechanics approach. Materials Letters, 78, pp. 154-158.

Mast, T.D. (2000) Empirical relationships between acoustic parameters in human soft tissues. Acoustic Research Letters Online. 1(2), pp. 37-42.

Morin, C. & Hellmich, C. A multiscale poromicromechanical approach to wave propagation and attenuation in bone. Ultrasonics. In Press, http://dx.doi.org/10.1016/j.ultras.2013.12.005.

NIST database www.nist.gov/pml/data/xraycoef

Sant, Z., Cauchi, M. & Spiteri, M. (2012) Analysis of stress-strain distribution within a spinal segment. Journal of Mechanics of Materials and Structures, 7(3), pp. 255-263.

Scheiner, S., Sinibaldi R., Pichler B., Komlev, V., Renghini, C., Vitale-Brovarone, C., Rustichelli, F. & Hellmich C. (2009) Micromechanics of bone tissue engineering scaffolds, based on resolution error-cleared computer tomography. Biomaterials, 30, pp. 2411-2419.

Vuong, J. & Hellmich, C. (2011) Bone fibrillogenesis and mineralization: Quantitative analysis and implications for tissue elasticity. Journal of Theoretical Biology, 287, pp. 115-130.